Original Research

Preventing Ethanol-Induced Brain and Eye Morphology Defects Using Optogenetics

Vaibhav P. Pai, PhD[1] and Dany Spencer Adams, PhD[2,3]

Abstract

Background: Embryonic exposure to the teratogen ethanol leads to dysmorphias, including eye and brain morphology defects associated with fetal alcohol spectrum disorder (FASD). Exposure of *Xenopus laevis* embryos to ethanol leads to similar developmental defects, including brain and eye dysmorphism, confirming our work and the work of others showing Xenopus as a useful system for studies of the brain and eye birth defects associated with FASD. Several targets of ethanol action have been hypothesized, one being regulation of *Kir2.1* potassium channel. Endogenous ion fluxes and membrane voltage variation (bioelectric signals) have been shown to be powerful regulators of embryonic cell behaviors that are required for correct brain and eye morphology. Disruptions to these voltage patterns lead to spatially correlated disruptions in gene expression patterns and corresponding morphology.
Materials and Methods: Here, we use controlled membrane voltage modulation to determine when and where voltage modulation is sufficient to rescue ethanol-induced brain and eye defects in Xenopus embryos.
Results: We found (1) that modulating membrane voltage using light activation of the channelrhodopsin-2 variant D156A rescues ethanol exposed embryos, resulting in normal brain and eye morphologies; (2) hyperpolarization is required for the full duration of ethanol exposure; (3) hyperpolarization of only superficial ectoderm is sufficient for this effect; and(4) the rescue effect acts at a distance.
Conclusions: These results, particularly the last, raise the exciting possibility of using bioelectric modulation to treat ethanol-induced brain and eye birth defects, possibly with extant ion channel drugs already prescribed to pregnant women. This may prove to be a simple and cost-effective strategy for reducing the impact of FASD.

Keywords: bioelectricity, *Xenopus*, fetal alcohol spectrum disorder, optogenetics, brain, eye, craniofacial development

Introduction

ABNORMAL NEURAL DEVELOPMENT causes highly debilitating disorders, such as spina bifida, and anencephaly,[1] brain malformations,[2] and susceptibility to autism and degenerative disorders such as Parkinson's and Alzheimer's disease.[3] Alcohol is a well-known teratogen that causes several neurological, craniofacial, and other morphological defects, as well as cognitive impairments, collectively referred to as fetal alcohol spectrum disorder (FASD[4–6]).

The most debilitating effects of alcohol are on neural tissue development leading to long-term cognitive and behavioral deficits.[4] Several molecular mechanisms have been shown to cause alcohol-associated teratogenic defects.[4–6] These mainly include ethanol-mediated dysfunction of ion channels and membrane voltage potentials,[5,7–10] metabotropic receptors (such as serotonin, cholinergic, and glutamate receptors),[11–13] retinoic acid signaling,[14–16] and reactive oxygen and nitrogen species signaling.[17–20] Finding repair strategies for such neural patterning defects is a crucial need in developmental medicine.

In addition to well-known genetic and biochemical signals, spatiotemporal changes in membrane voltage across somatic cells (bioelectric signals) regulate many aspects of large-scale embryonic patterning.[21–28] Channelopathies,[29] syndromes developing from mutations in ion channel genes, often cause brain and eye anomalies, strongly implicating bioelectricity as an important regulator of brain and eye development. Using voltage-sensitive dyes,[30] developing *Xenopus* embryos were shown to have dynamic spatiotemporal changes in the ectodermal membrane voltage now known as the ''electric face.''[31] Inhibiting or misexpressing channels that normally

[1]Department of Biology, Tufts Center for Regenerative and Developmental Biology, Tufts University, Medford, Massachusetts.
[2]Department of Biology, Tufts University, Medford, Massachusetts.
[3]Ion Diagnostics LLC, Watertown, Massachusetts.

regulate membrane voltage, such as Kir2.1[24] and the proton-pumping complex H$^+$-VATPase,[31] disrupt craniofacial morphogenesis, including brain and eye patterning.[31–35]

All these tissues are derivatives of anterior ectodermal cells in neural crest and placode lineages.[36–41] The specific embryonic membrane voltage patterns that regulate eye and brain patterning are so powerful that they can induce ectopic (and functional) eye and brain tissue far outside the head region (even in the tail of the animal).[32,34] These bioelectric signals operate upstream and control the canonical transcription factors and gene regulator networks involved in eye and brain patterning.[32–35] Moreover, reinforcing these endogenous membrane voltage patterns rescues eye and brain defects caused by mutant notch and teratogen nicotine.[34,42,43] These experiments show that the bioelectric prepattern is necessary and sufficient for normal eye and brain morphogenesis as well as normal expression of the patterning genes.

Here we test the hypothesis that bioelectric signal modulation can also rescue ethanol-induced brain and eye morphology defects. We use optogenetics, light-mediated regulation of ion channel function and ion fluxes,[44–46] to achieve spatiotemporal control of bioelectric signal modulation. Such optogenetic modulation of bioelectric signal in nonexcitable cells has been used in *Xenopus* tail regeneration and cancer.[47,48] Successful optogenetic rescue of ethanol-induced brain and eye defects would suggest that preventive medical approaches may not require gene therapy or replacement of a particular protein or protein complex; rather, rescue may be accomplished with one of the many extant methods for modulating bioelectric signals.

Here we confirm that ethanol exposure induces severe brain and eye patterning defects in *Xenopus,* as reported,[6,18,49,50] Next, we used the optogenetic reagent ChR2^{D156A}, to generate corrective bioelectric signals, to prevent ethanol-induced brain and eye morphology defects. This bioelectric modulation was required for the full duration of ethanol exposure to bring about the rescue effect; activity of ChR2^{D156A} only during portion of ethanol exposure (stage 9–23 or stage 23–40) was not sufficient.

Interestingly, ChR2^{D156A}-mediated bioelectric modulation was successful regardless of whether the ChR2^{D156A} was expressed dorsally (colocalized with precursors of brain and eye—local expression) or ventrally (distant—nonlocal expression), indicating that these corrective signals can act locally or at a distance. This suggests the possibility of preventing FASD-related brain and eye morphological defects without the need to carefully target a specific set of embryonic cells. This would dramatically reduce the difficulty and cost of preventing of these devastating defects in humans.

Methods and Materials

Xenopus husbandry

Xenopus laevis embryos were fertilized *in vitro* according to standard protocols[51] and raised in 0.1×Marc's Modified Ringer's (MMR; 10 mM Na$^+$, 0.2 mM K$^+$, 10.5 mM Cl$^-$, 0.2 mM Ca^{2+}, pH 7.8). Embryos were housed at 14°C overnight after injection and subsequently at 18°C, and staged according to Refs.[52,53] We saw the normal, low background levels of brain and eye anomalies (<9%), indicating good animal health and good rearing conditions. At stage 45, large-scale brain and eye patterning and anomalies in gross morphology were as-

sessed as before[32,34,42] and using Refs.[18,49,50,52,54] All experiments were approved by the Tufts University Animal Research Committee (Protocol M2017–53A) in accordance with the Guide for Care and Use of Laboratory Animals.

Microinjections

Capped synthetic mRNAs generated using the mMES-SAGE mMACHINE kit (Ambion) were dissolved in nuclease-free water and injected into embryos immersed in 3% Ficoll using standard methods.[51] Each injection was delivered between 0.5 and 1 ng of mRNA to each cell at the two-cell stage; the needle was aimed toward the middle of each cell at the animal pole, using standard methods.

Constructs used were *ChR2^{D156A}*[55] and *β-galactosidase* in pCS2. Embryos were injected with capped mRNA in following ways: both the blastomeres at two-cell stage, dorsal two blastomeres at four-cell stage, or ventral two blastomeres at four-cell stage. Embryos were injected in 3% Ficoll solution and after 30 min were washed and reared in 0.1×MMR until stage 45.

β-galactosidase enzymatic detection

Embryos injected with lineage tracer *β-galactosidase* mRNA were reared to stage 45 and fixed (30 min in Modified Eagle's Medium with formalin at room temperature), washed twice in phosphate-buffered saline (PBS) with 2 mM MgCl$_2$, and stained with X-gal (Roche Applied Sciences, Indianapolis, IN) staining solution at 37°C for 3 h. Embryos were then rinsed three times in PBS and analyzed.

Optogenetics

We used a modified channelrhodopsin-2, ChR2^{D156A} (a nonspecific cation channel[45,55,56]), because of its high channel open time[55] and low incidence of side effects in *Xenopus* embryos where it has been characterized.[48,57] ChR2^{D156A} has been characterized in detail elsewhere and shown to act as a hyperpolarizer in the outer ectoderm of *Xenopus* embryos due to very low osmolarity of 0.1×MMR.[57,58] A fluorescent tag reported *ChR2^{D156A}* expression; only embryos with clear expression were used as controls or in experiments. To illuminate embryos with 450 nm light, embryos in 35-mm plastic Petri dishes were placed in a 12″×12″×10″ custom-made, light-tight box (Boston Engineering, Waltham, MA).

Two computer-controlled SugarCUBE™ LED Illumination Systems (Ushio) supplied light through fiberoptic cables that feed into the box through the top. To prevent overheating, dishes were placed on a water-cooled stage. Dishes were exposed to a previously determined optimal light exposure regimen, 10 ms on and then 30 s off. The intensity of the light reaching the dishes during the "on" phase was found to be 2.4±0.1 mW/mm^2 at approximately the height of the embryos. This blue light regimen alone has no effect on normal, wild-type embryos.[57]

Ethanol exposure

Embryos were moved to 35-mm Petri dishes containing 2% ethanol in 0.1×MMR. The dishes were then moved to the light-tight box, either covered (control) or uncovered, or returned to the 18°C incubator to incubate in dark conditions (control). *Xenopus* embryos were exposed to 2% ethanol in three regimens associated with neural development: early

(stage 9–23), late (stage 23–40), and full (stage 9–40). Brain and eye morphology of these embryos was assessed after they had developed to stage 45 (Fig. 1).

Statistics

All statistical analyses were performed using Microsoft Excel. At least three independent experiments ($n > 3$) were conducted with $N \geq 25$ embryos for each experimental group, with embryos collected from multiple animals across independent clutches. After confirming equal variance of the replicate samples, data were pooled and analyzed using a χ^2 test for differences in proportions.

Results

Exposure to 2% ethanol during neurula and tailbud stages induces brain and eye defects

In experiments to test the effects of 2% ethanol on tadpole neural development, 97% of untreated control tadpoles had
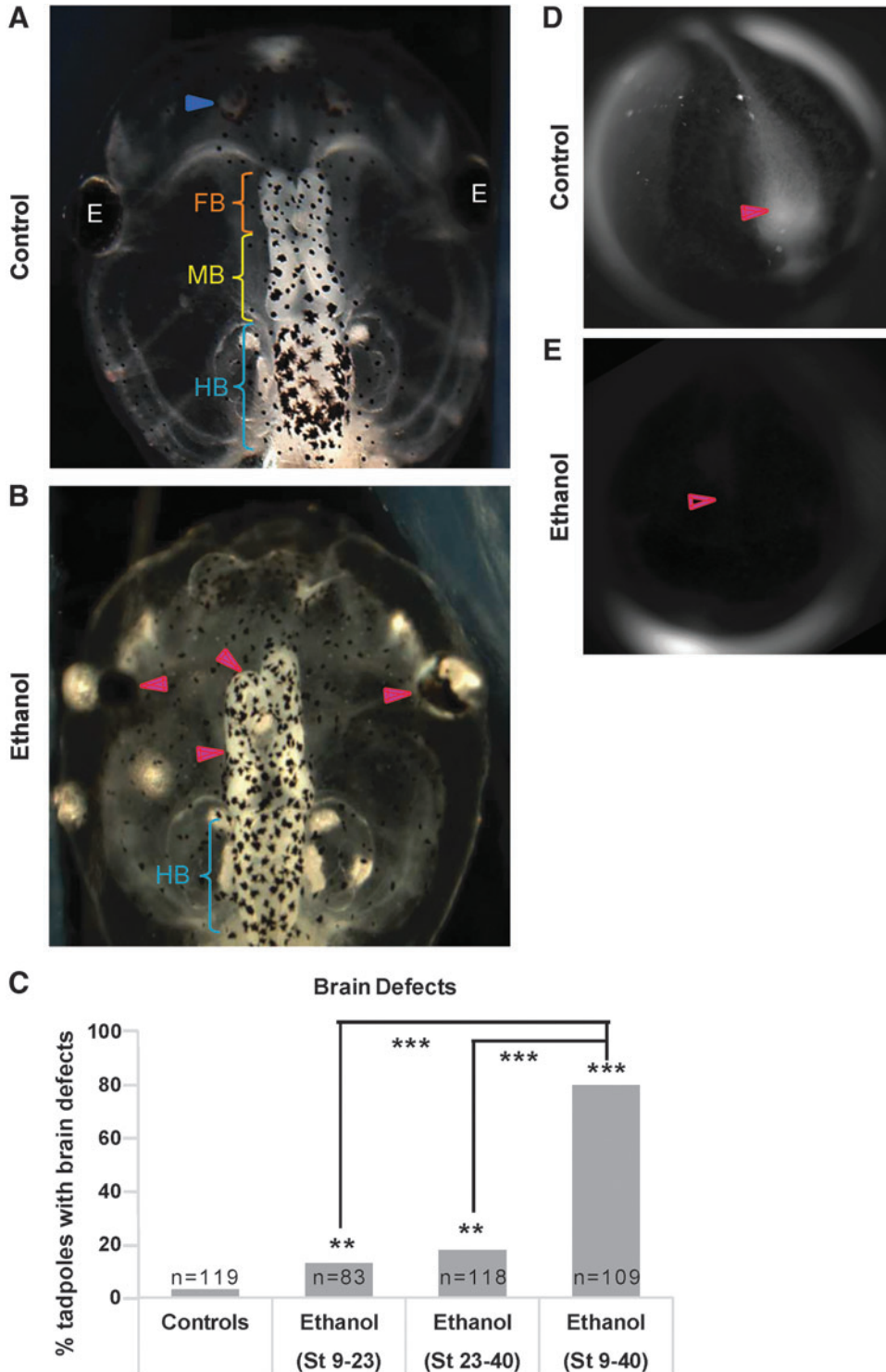

FIG. 1. Ethanol induces brain morphology defects in *Xenopus* embryos. Representative images of stage 45 tadpoles: **(A)** control tadpoles showing nostrils (blue arrowheads), FB indicated by the orange bracket, MB indicated by the yellow bracket, and HB indicated by the cyan bracket. **(B)** Tadpoles from embryos exposed to ethanol (2%—stage 9–40) showing severe brain morphology defects as indicated by magenta arrowheads. Cyan brackets indicate presence of HB. **(C)** Quantification of stage 45 tadpoles for major brain morphology phenotypes in the absence or presence of ethanol (2%). A significantly high incidence of malformed brain was observed in embryos exposed to ethanol for the full duration (stage 9–40) in comparison with controls. Ethanol (2%) exposure for shorter durations—stage 9–23 and stage 23–40—also showed an increase in malformed brains, relative to untreated controls, but the incidence of malformed brains in shorter ethanol exposures was significantly lower than in full ethanol exposure. Data were pooled and a χ^2 test was performed; ***$p < 0.001$, **$p < 0.001$. Representative CC2-DMPE images of stage ~15 *Xenopus* embryos: **(D)** untreated controls and **(E)** ethanol-exposed (2%, stage 9–40). Control embryos show characteristic hyperpolarization in the neural plate (solid magenta arrows) as previously reported.[34,42] Ethanol-treated embryos showed significantly reduced signal (depolarization) within the neural plate (hollow magenta arrows). FB, forebrain; HB, hindbrain; MB, midbrain.

correctly patterned large-scale gross morphology of brain and eye tissue,[18,32,50,52,54] with well-formed eyes, nostrils, olfactory bulbs/forebrain, midbrain, and hindbrain (Fig. 1A, C). In comparison, early (stage 9–23) and late (stage 23–40) ethanol (2%) exposure regimens both caused a small but significant increase in incidence of brain and eye morphology defects (13% and 18%, respectively, compared with 3% of controls, $p < 0.01$; Fig. 1B, C). The full ethanol exposure regimen (stage 9–40) resulted in a pronounced increase in incidence of brain and eye morphology defects relative to the shorter exposures (80%, $p < 0.001$) (Fig. 1C).

The most striking brain phenotypes were misformed or absent nostrils, mispatterned forebrain and midbrain (Fig. 1B). Hindbrain gross morphology was largely unaffected. The most striking eye phenotypes were small eyes and/or incompletely formed eyes, pigmented optic nerve, and fusion of eyes to brain (Fig. 1B). Eye development was more sensitive to ethanol exposure than brain development. We conclude that stage 9–40 ethanol (2%) exposure was most penetrant in inducing brain and eye phenotypes and therefore used this exposure regimen for the remaining experiments.

Light activation of the ChR2D156A channel rescues ethanol-induced brain and eye morphology defects

We tested whether optogenetic modulation of membrane voltage can rescue ethanol-induced brain and eye morphology defects. We used a modified channelrhodopsin-2, ChR2[D156A]. Our conditions were examined: uninjected controls, with and without ethanol, and *ChR2[D156A]*-injected (both blastomeres at two-cell stage to obtain expression throughout) embryos that were divided into two groups—ethanol + blue light and ethanol + dark (*ChR2[D156A]* activity control). Embryos were allowed to develop to stage 45 and their brain and eye morphology was assessed (Fig. 2). Uninjected, untreated tadpoles had correctly patterned brain and eye tissues,[54] including normally developed eyes, nostrils, olfactory bulbs, forebrain, midbrain, and hindbrain (Fig. 2A, D). As before (Fig. 1), ethanol exposure caused a significantly high incidence of brain and eye morphology defects (80%, $p < 0.001$) in comparison with untreated controls (5%; Fig. 2D). *ChR2[D156A]*

mRNA-injected, ethanol-treated embryos that were kept in dark (ChR2[D156A] channels not activated) also showed a significantly higher incidence of brain and eye morphology defects (90%, $p < 0.001$) (Fig. 2B, D). Excitingly, *ChR2[D156A]* mRNA-injected, ethanol-treated embryos that were exposed to blue light (ChR2[D156A] channels activated) showed significant rescue of brain and eye morphology defects relative to ethanol exposed, ChR2[D156A] expressing, but kept in the dark (25%, $p < 0.001$; Fig. 2C, D). The rescued tadpoles showed normal eyes, nostrils, forebrain, midbrain, and hindbrain, similar to the controls (Fig. 2C). Thus, blue light activation of ChR2[D156A] channels restored normal brain and eye morphology of ethanol-treated embryos to the wild-type state.

Next we tested whether the rescue of ethanol-induced brain defects could be due to blue light alone, or injection and blue light. Four conditions were examined: uninjected untreated controls, ethanol-treated embryos, ethanol-treated embryos that were exposed to blue light, and ethanol-treated embryos that were microinjected with *β-galactosidase* mRNA in both blastomeres at two-cell stage and exposed to blue light. Embryos were allowed to develop to stage 45 and their brain and eye morphology was assessed (Fig. 2E).

Uninjected and untreated tadpoles had correctly patterned brain and eye tissues, including normally developed eyes, nostrils, olfactory bulbs, forebrain, midbrain, and hindbrain (Fig. 2E). Ethanol exposure caused a significant increase in the incidence of brain and eye morphology defects (81%, $p < 0.001$) in comparison with untreated controls (4%, Fig. 2E). Ethanol-treated embryos that were exposed to blue light also showed a significant increase in the incidence of brain and eye morphology defects (84%, $p < 0.001$) in comparison with controls (Fig. 2E). Similarly, ethanol-treated embryos that were injected with *β-galactosidase* mRNA and exposed to blue light also showed a significant increase in the incidence of brain and eye morphology defects (71%, $p < 0.001$) in comparison with controls (Fig. 2E). There was no significant difference between ethanol-treated, ethanol-treated and blue light exposed, and ethanol-treated, *β-galactosidase* mRNA-injected, blue light-exposed tadpoles (Fig. 2E). These results suggest that it is the blue light activation of ChR2[D156A] channels that restored normal brain and eye morphology of ethanol-treated embryos.

FIG. 2. Optogenetic activation of channel rhodopsin (ChR2[D156A]) rescues ethanol-induced brain morphology defects in *Xenopus* embryos. Representative images of stage 45 tadpoles: **(A)** control tadpole showing nostrils (blue arrowheads), FB indicated by the orange bracket, MB indicated by the yellow bracket, and HB indicated by the cyan bracket, **(B)** tadpole from embryos exposed to ethanol (2%—stage 9–40) and microinjected with channel rhodopsin (*ChR2[D156A]*) mRNA in both blastomeres at two-cell stage, showing severe brain morphology defects as indicated by magenta arrowheads. Cyan brackets indicate presence of HB, **(C)** tadpole from embryos exposed to ethanol (2%—stage 9–40), microinjected with channel rhodopsin (*ChR2[D156A]*) mRNA in both blastomeres at two-cell stage, and exposed to blue light (stage 9–40), showing restoration of brain pattern with intact nostrils (blue arrowheads), distinct FB (orange bracket), MB (yellow bracket), and HB (cyan brackets). **(D)** Quantification of tadpoles with malformed brain phenotype in control (untreated and uninjected) embryos, embryos exposed to ethanol (2%—stage 9–40) with microinjection with channel rhodopsin (*ChR2[D156A]*) mRNA in both blastomeres at two-cell stage. A subset of ethanol-exposed, rhodopsin microinjected embryos were exposed to blue light (stage 9–40) for optogenetic activation of the channel rhodopsin. Ethanol exposure results in malformed brain phenotype and this effect of ethanol is not affected by channel rhodopsin microinjection. Remarkably, exposure to blue light significantly rescues this effect of ethanol. Data were pooled and a χ^2 test was performed; ***$p < 0.001$, **$p < 0.001$. **(E)** Quantification of tadpoles with malformed brain phenotype in control (untreated and uninjected) embryos and embryos exposed to ethanol (2%—stage 9–40). A subset of ethanol exposed embryos were exposed to blue light (stage 9–40) as controls. Another subset of ethanol exposed embryos were microinjected with *β-galactosidase* mRNA in both blastomeres at two-cell stages and exposed to blue light (stage 9–40) as controls. Ethanol exposure results in malformed brain phenotype and this effect of ethanol is not affected by blue light or *β-galactosidase* mRNA + blue light. Data were pooled for greater than three experiments, and a χ^2 test was performed; ***$p < 0.001$. n.s., nonsignificant.

*Light activation of ChR2^{D156A} channel for the full
duration of ethanol exposure is necessary for rescue
of brain and eye morphology defects*

To determine whether opening of ChR2^{D156A} channels is
required throughout the full duration of ethanol exposure or if
shorter exposure can have preventative or curative effects, we
repeated the above experiment with three different blue light

exposure regimens. Controls again had correctly patterned
brain and eye tissues (Fig. 2A, E). Also as before, ethanol
exposure caused a significantly higher incidence of brain and
eye morphology defects (78%, $p < 0.001$; Fig. 3B, E), and
ChR2^{D156A} mRNA-injected, ethanol-treated embryos ex-
posed to light for the full duration of ethanol exposure
showed significant rescue of brain and eye morphology de-
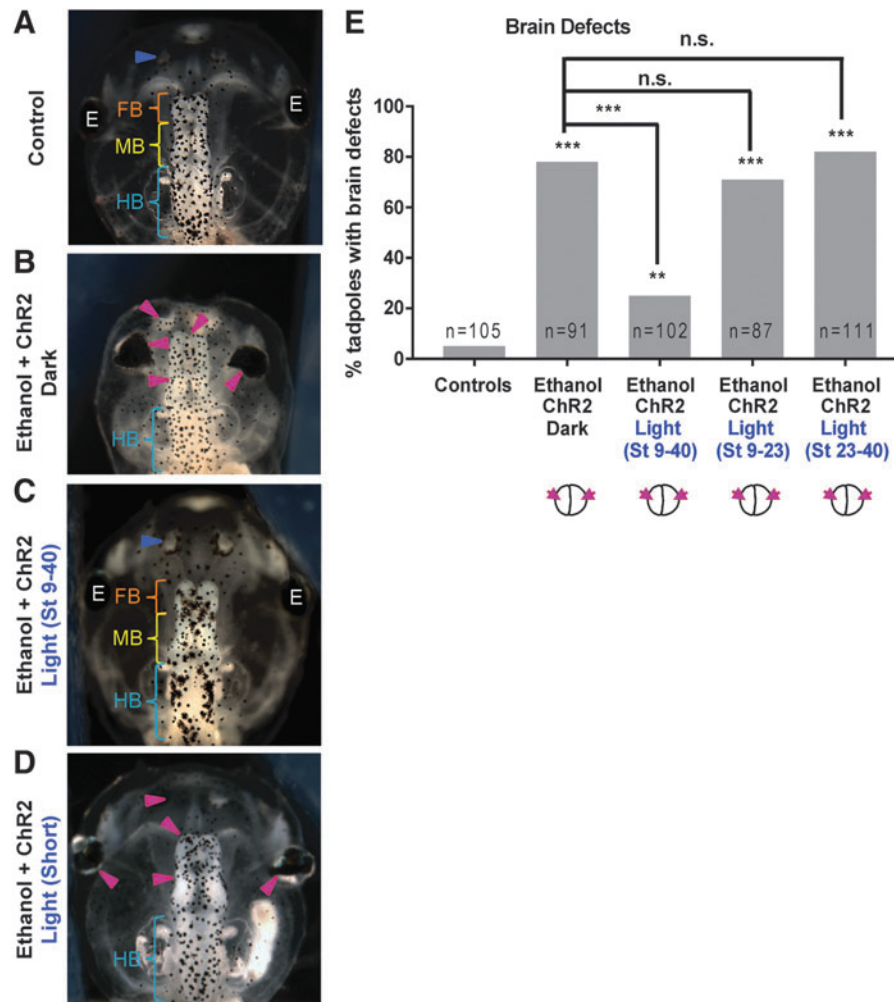fects (26%, $p < 0.001$) (Fig. 3C, E). However, blue light
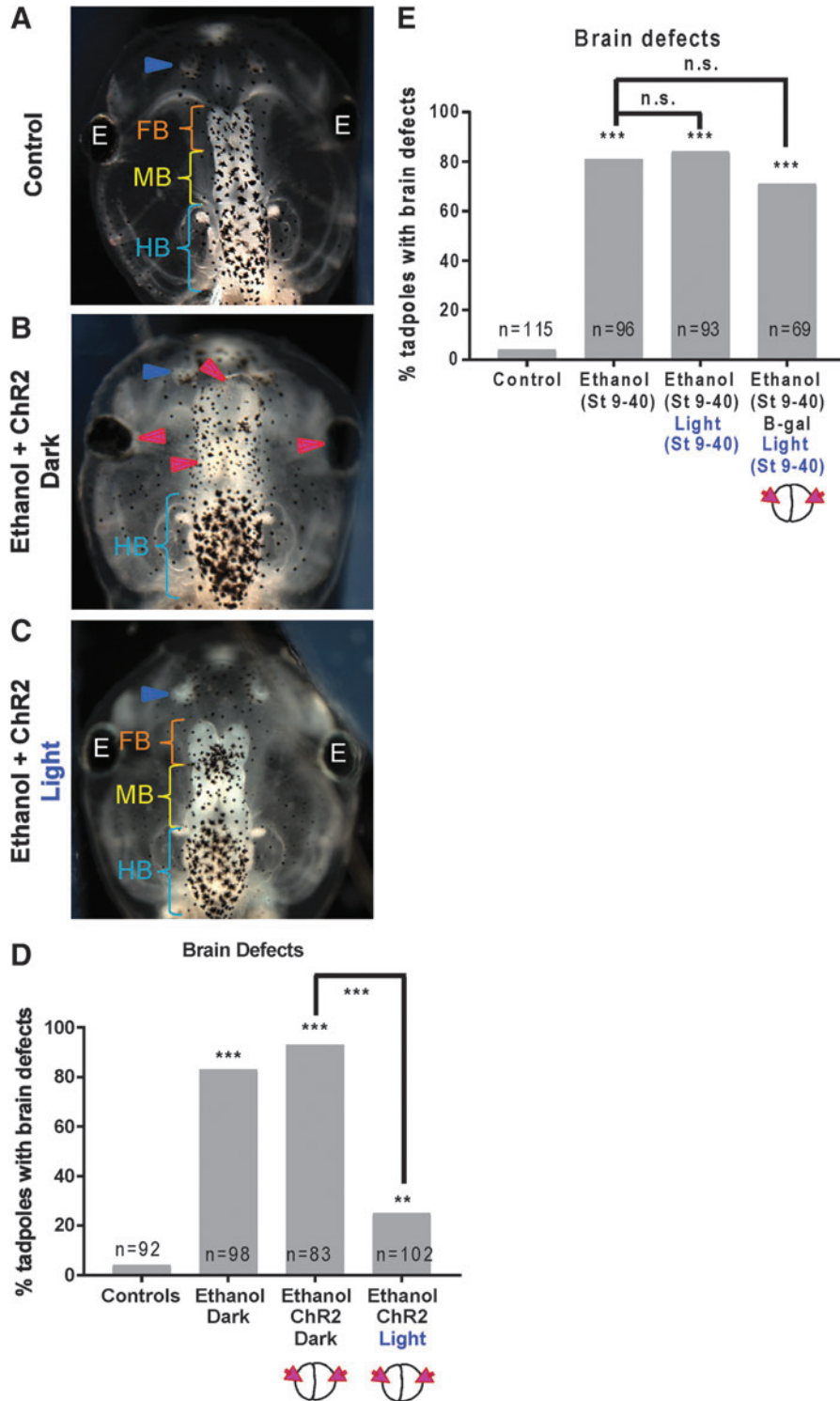
FIG. 3. Optogenetic activation of channel rhodopsin (ChR2[D156A]) for a short duration does not rescue ethanol-induced brain morphology defects in *Xenopus* embryos. Representative images of stage 45 tadpoles: **(A)** control tadpole showing nostrils (blue arrowheads), FB indicated by the orange bracket, MB indicated by the yellow bracket, and HB indicated by the cyan bracket, **(B)** tadpole from embryos exposed to ethanol (2%—stage 9–40) and microinjected with channel rhodopsin (*ChR2[D156A]*) mRNA in both blastomeres at two-cell stage, showing severe brain morphology defects as indicated by magenta arrowheads. Cyan brackets indicate unaffected HB, **(C)** tadpole from embryos exposed to ethanol (2%—stage 9–40), microinjected with channel rhodopsin (*ChR2[D156A]*) mRNA in both blastomeres at two-cell stage, and exposed to blue light (stage 9–40), showing restoration of brain pattern with intact nostrils (blue arrowheads), distinct FB (orange bracket), MB (yellow bracket), and HB (cyan brackets), **(D)** tadpole from embryos exposed to ethanol (2%—stage 9–40), microinjected with channel rhodopsin (*ChR2[D156A]*) mRNA in both blastomeres at two-cell stage, and exposed to blue light for a shorter duration (stage 9–23 or stage 23–40), showing brain morphology defects as indicated by magenta arrowheads. Cyan brackets indicate unaffected HB. **(E)** Quantification of tadpoles with malformed brain phenotype in control (untreated and uninjected) embryos, embryos exposed to ethanol (2%—stage 9–40) with microinjection of channel rhodopsin (*ChR2[D156A]*) mRNA in both blastomeres at two-cell stage. A subset of ethanol-exposed, rhodopsin microinjected embryos were exposed to blue light (stage 9–40) for optogenetic activation of the channel rhodopsin. A second and third subset of these embryos were exposed to blue light for shorter time periods to time—stage 9–23 and stage 23–40, respectively. Ethanol exposure results in malformed brain phenotype and this effect of ethanol is not affected by channel rhodopsin microinjection. Blue light-mediated activation of channel rhodopsin (stage 9–40) significantly rescues this effect of ethanol. Interestingly, blue light-mediated activation of channel rhodopsin for a shorter duration—stage 9–23 and stage 23–40—fails to show the rescue effect. Data were pooled and a χ^2 test was performed; ***$p < 0.001$, **$p < 0.001$.

exposure for short durations, stages 9–23 or stages 23–40, failed to show significant rescue of brain and eye morphology (71% and 82%, respectively) (Fig. 3D, E). Thus, optogenetic activation of ChR2[D156A] channels restored normal brain and eye morphology of ethanol-treated embryos only when the channels are opened throughout the duration of ethanol exposure.

Light activation of the ChR2[D156A] channel rescues ethanol-induced brain and eye morphology defects through both local and nonlocal effects

To discover whether the ChR2[D156A] rescue of ethanol-induced brain and eye defects occurs in a local or nonlocal (noncell autonomous) manner, we targeted the mRNA to
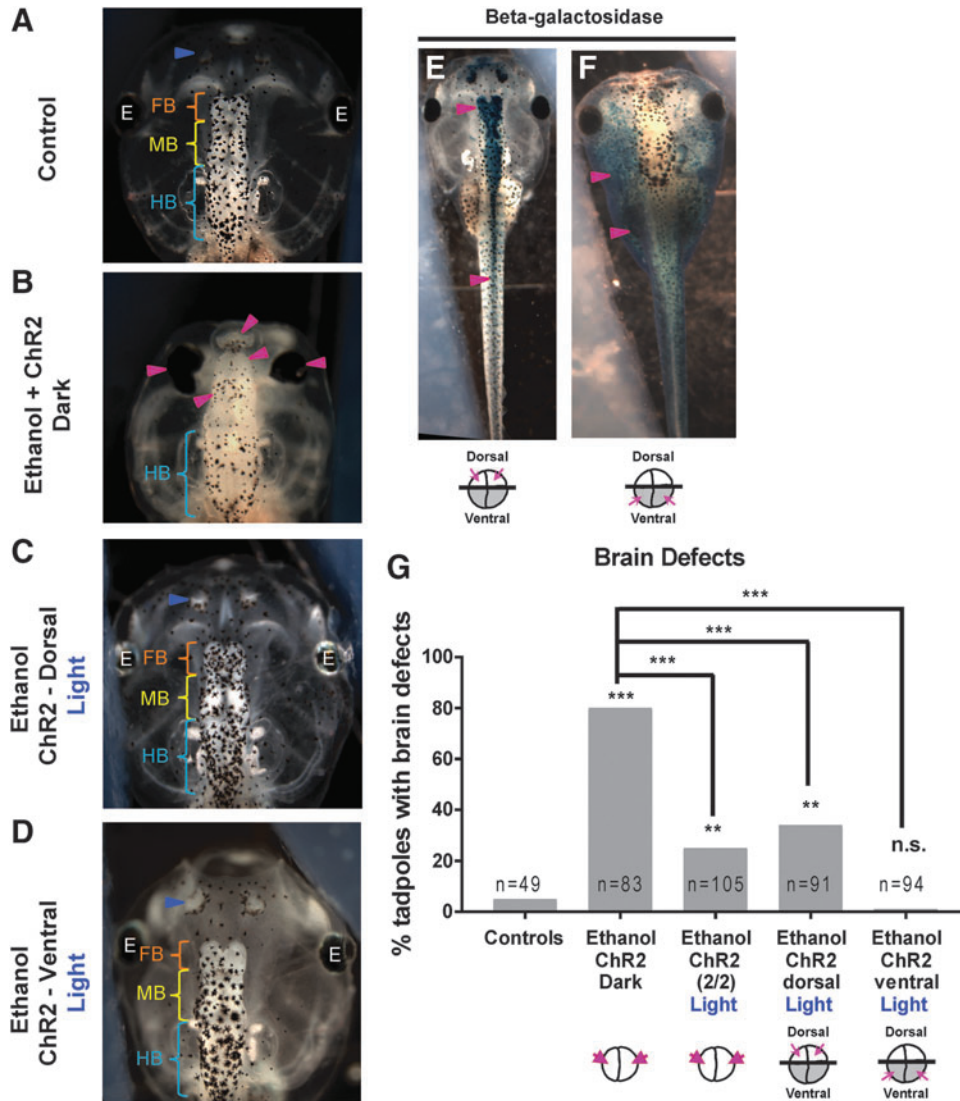
FIG. 4. Optogenetic activation of channel rhodopsin (ChR2^{D156A}) rescues ethanol-induced brain morphology defects through local and nonlocal effects in *Xenopus* embryos. Representative images of stage 45 tadpoles: **(A)** control tadpole showing nostrils (blue arrowheads), FB indicated by the orange bracket, MB indicated by the yellow bracket, and HB indicated by the cyan bracket, **(B)** tadpole from embryos exposed to ethanol (2%—stage 9–40) and microinjected with channel rhodopsin (*ChR2^{D156A}*) mRNA in both blastomeres at two-cell stage, showing severe brain morphology defects as indicated by magenta arrowheads. Cyan brackets indicate unaffected HB, **(C)** tadpole from embryos exposed to ethanol (2%—stage 9–40), microinjected with channel rhodopsin (*ChR2^{D156A}*) mRNA in dorsal two blastomeres at four-cell stage, and exposed to blue light (stage 9–40), showing restoration of brain pattern with intact nostrils (blue arrowheads), distinct FB (orange bracket), MB (yellow bracket), and HB (cyan brackets), **(D)** tadpole from embryos exposed to ethanol (2%—stage 9–40), microinjected with channel rhodopsin (*ChR2^{D156A}*) mRNA in ventral two blastomeres at four-cell stage, and exposed to blue light (stage 9–40), showing restoration of brain pattern with intact nostrils (blue arrowheads), distinct FB (orange bracket), MB (yellow bracket), and HB (cyan brackets). **(E)** Tadpole from embryos coinjected with channel rhodopsin *ChR2^{D156A}* and lineage tracer *β-galactosidase* mRNA in the dorsal two blastomeres at four-cell stage. *β-galactosidase* stain was developed using X-gal (deep blue stain), which was observed mainly in the brain and spinal cord (magenta arrowheads) indicating that dorsal blastomere injections target neural tissues. **(F)** Tadpole from embryos coinjected with channel rhodopsin *ChR2^{D156A}* and lineage tracer *β-galactosidase* mRNA in the ventral two blastomeres at four-cell stage. *β-galactosidase* stain was developed using X-gal (deep blue stain), which was absent from the brain and spinal cord, and mainly present in brachial arches, gut, heart, and muscles (magenta arrowheads) indicating that ventral blastomere injections target non-neural tissues. **(G)** Quantification of tadpoles with malformed brain phenotype in control (untreated and uninjected) embryos, embryos exposed to ethanol (2%—stage 9–40) with microinjection of channel rhodopsin (*ChR2^{D156A}*) mRNA in both blastomeres at two-cell stage. A subset of ethanol-exposed, channel rhodopsin microinjected embryos were exposed to blue light (stage 9–40) for optogenetic activation of the channel rhodopsin. A second and third subset of these embryos exposed to ethanol were microinjected with channel rhodopsin (*ChR2^{D156A}*) mRNA at four-cell stage in either dorsal two blastomeres (targets neural tissues) or ventral two blastomeres (excludes the neural tissues), respectively. Ethanol exposure results in malformed brain phenotype. Blue light-mediated activation of channel rhodopsin (stage 9–40) significantly rescues this effect of ethanol in embryos that received channel rhodopsin in both blastomeres at two-cell stage and embryos that received channel rhodopsin in dorsal two blastomeres (neural precursors) at four-cell stage. Remarkably, blue light-mediated activation of channel rhodopsin in embryos that received channel rhodopsin in ventral two blastomeres (non-neural precursors) showed the best rescue from effect of ethanol on brain morphology. Data were pooled and a χ^2 test was performed; ***$p < 0.001$, **$p < 0.001$.

dorsal two cells at four-cell stage (precursors of neural tissue[59]) or ventral two cells at four-cell stage (precursors not contributing to neural tissue[59]) of the embryo. We confirmed the precision of this targeting using coinjection of lineage tracer *β-galactosidase* mRNA followed by X-gal staining and imaging (Fig. 4E, F). Greater than ninety percent of dorsal-blastomere microinjected tadpoles showed X-gal stain mainly in the brain and spinal cord confirming targeting of the ChR2[D156A] channels to the neural tissues, as desired (Fig. 4E). Greater than ninety percent of ventral-blastomere microinjected tadpoles showed X-gal stain present in the gut, heart, and muscles, but absent in the brain and spinal cord, suggesting targeting of ChR2[D156A] channels to the non-CNS ventral tissues (Fig. 4F).

For the experiment, *ChR2[D156A]* mRNA was microinjected into either dorsal or ventral blastomeres at four-cell stage, and then, the embryos were treated with 2% ethanol as before (stage 9–40) and allowed to develop to stage 45 when their brain and eye morphology was assessed (Fig. 4). Control (untreated uninjected) tadpoles had correctly patterned brain and eye tissues,[54] including normally developed eyes, nostrils, olfactory bulbs, forebrain, midbrain, and hindbrain (Fig. 4A, G). *ChR2[D156A]* mRNA microinjected (in both blastomeres at two-cell stage), ethanol-treated embryos that were kept in the dark (ChR2[D156A] channels not activated) showed a significantly higher incidence of brain and eye morphology defects (81%, $p < 0.001$) than controls (6%) (Fig. 4B, G). *ChR2[D156A]* mRNA microinjected (in both blastomeres at two-cell stage), ethanol-treated embryos that were exposed to the full (stage 9–40) blue light regimen (ChR2[D156A] channels activated) showed significant rescue of brain and eye morphology defects (23%, $p < 0.001$) (Fig. 4G). Interestingly, dorsally injected (ChR2[D156A] expression in the CNS precursors), ethanol-treated embryos that were exposed to the full blue light regimen (ChR2[D156A] channels activated) also showed significant rescue of brain and eye morphology

defects (34%, $p < 0.001$) (Fig. 4C, G). Unexpectedly and remarkably, ventrally injected (ChR2[D156A] expression not in the CNS precursors), ethanol-treated embryos that were exposed to the full blue light regimen (ChR2[D156A] channels activated) showed the best rescue of brain and eye morphology defects (1%, $p < 0.001$) (Fig. 4D, G). These results provide evidence that the ChR2[D156A]-mediated bioelectric rescue operates locally as well as nonlocally.

Discussion

In addition to well-known genetic and biochemical pathways, spatiotemporal changes in bioelectric signals, such as ion flux and membrane voltage of cells, have been shown to regulate aspects of large-scale patterning during embryonic development.[60–65] In addition to sculpting neural connections during embryonic development,[66,67] bioelectric signals control important aspects of large-scale morphogenesis of the eye and brain, as summarized in Figure 5.[31–35,68] Reinforcing correct bioelectrical signals has been shown to rescue neural patterning defects caused by aberrant notch signals, mechanical damage, or exposure to neuro-teratogens such a nicotine.[34,42,43]

Our previous work has extended the use of optogenetics to embryonic and regenerating tissues to more accurately control the timing and location of bioelectric intervention,[47,48] thus increasing our resolution as we study the intertwining of bioelectric events with second messengers and genetic regulatory networks. Building on these findings, we investigated optogenetic modulation of bioelectric signals for rescue of brain and eye malformations in a *Xenopus* model of fetal alcohol syndrome disorder.[4–6] Here we do not intend to investigate the mechanisms used by ethanol to induce brain and eye defects, which are well studied and established,[4–7,10,11,13,20] but use ethanol as an established teratogen to assess the ability of optogenetic membrane-voltage modulation to rescue ethanol-induced brain and eye patterning defects.

FIG. 5. Schematic of bioelectric signaling in neural teratogenesis and repair. **(A)** Summary of our previous studies.[34,42] showing hyperpolarized neural plate and depolarized surrounding ectoderm as important regulators of proper brain and eye morphology. **(B)** Embryonic ethanol exposure depolarizes the neural plate leading to aberrant brain and eye morphology defects. **(C)** Adding hyperpolarizing ChR2-D156A channel into the ethanol-treated embryos with subsequent blue light exposure to optogenetically open the channel may be sufficient to prevent the depolarizing effect of ethanol leading to normal brain and eye morphology.
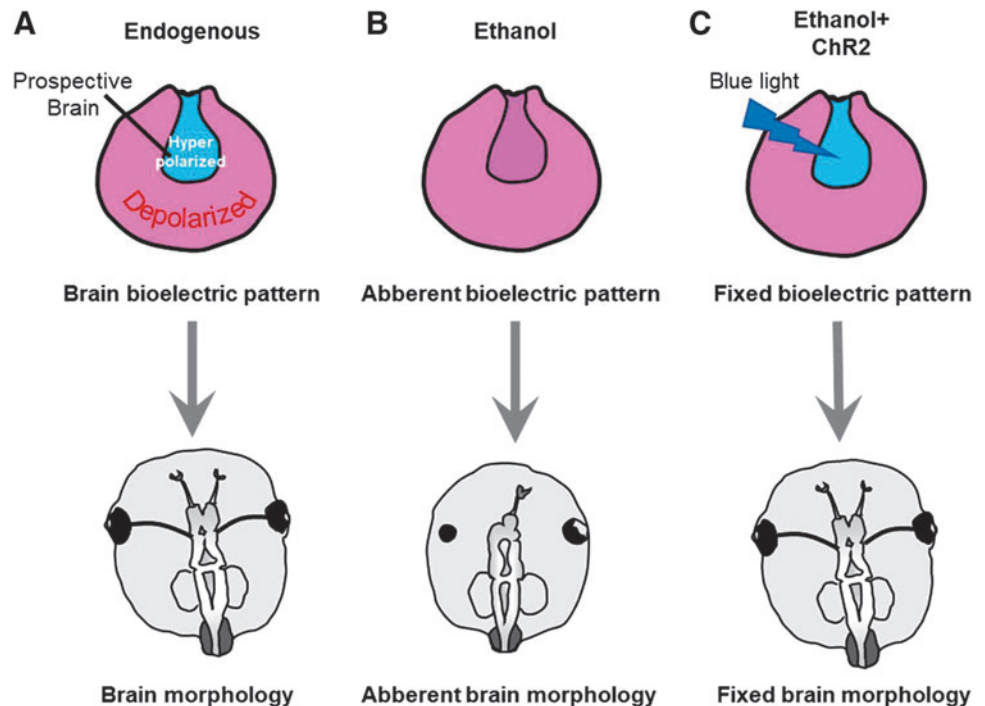
Among the various optogenetic channels tested in *Xenopus*,[57] the channelrhodopsin-2 variant ChR2[D156A] was used because it has been shown to hyperpolarize the membrane[48,57] with fewest side effects during embryogenesis. Using electrophysiology and membrane voltage reporter dyes, we have shown that ChR2[D156A] hyperpolarizes cells in *Xenopus* embryos.[48,57] Unlike mammalian cells where ChR2[D156A] depolarizes the cell, in *Xenopus* the cation concentrations are extremely low in the $0.1 \times$ MMR medium resulting in a net cation gradient that drives cations out of the ectodermal cells throughout early developmental stages (until stage 35). Also, in *Xenopus* embryos, the heart and circulatory system do not become operational until later developmental stages (poststage 35)[69]; thus resulting in the ChR2[D156A] channel opening leading to hyperpolarization during early development (prestage 35). This hyperpolarizing action of ChR2[D156A] in *Xenopus* embryos has been verified with electrophysiology and voltage reporter dye imaging.[48,57]

The activating blue light cannot penetrate deeper than the outer opaque ectodermal layer, resulting in activation of channels and hyperpolarization only in these outer ectodermal cells. Nonetheless, although ChR2[D156A] hyperpolarizes ectodermal *Xenopus* embryonic cells, it is also possible that the change in internal ionic concentration of these cells (due to cation efflux) results in initiation/inhibition of signaling events.[70–72] In such a case, the effect of opening ChR2[D156A] could be independent of its effect on membrane potential. Although such effects have not been reported in embryonic development and are less likely, this possibility cannot be ruled out and will be tested in future by using different ion-type channels.

Desensitization of ChR2[D156A] upon blue light exposure was not a problem as we are not looking at fast spiking neuronal activity; we are inducing slow, long-lasting changes in membrane potential, such as those found in embryonic cells.[57] Also, exposure to blue light was limited to 10 s pulses followed by 30 s in darkness, a regimen shown to work in *Xenopus*, to minimize desensitization and to prevent overheating of the medium.[47,57,73]

To maximize the effect of ethanol on neural patterning and minimize other non-neural effects, we exposed *Xenopus* embryos to ethanol during neurulation and tailbud stages from stage 9–40. We observed major mispatterning of neural tissue (Fig. 1) as has been demonstrated in previous studies.[6,49] We also tried two short regimens of ethanol exposure (stage 9–23 and stage 23–40) to discover the minimal levels of ethanol exposure required. Surprisingly, neither of the short regimens induced as severe neural patterning defects as the full regimen (stage 9–40) (Fig. 1). This suggested that ethanol exposure throughout these stages is required for inducing severe neural patterning defects.

Exposure to ethanol during the developmental stages that are sensitive to depolarization by other means (stage 9–23) is not sufficient to cause brain and eye anomalies. This was an unexpected and intriguing result, suggesting that the brain and eye symptoms associated with fetal alcohol syndrome are different from those associated with expression of the *Kir2.1* variants that cause brain and eye symptoms in Andersen-Tawil patients.[5,24] One explanation could be that Kir2.1 variants are more stably inhibited by mutations than ethanol inhibition of Kir2.1. Periodic unbinding of ethanol would allow some Kir2.1 channels to function normally for some of the critical time. If true, this explanation predicts that there is a threshold effect that causes the anomalies, and the more consistent Kir2.1 mutants reach that threshold faster than the more sporadic ethanol effects. In addition to Kir2.1, ethanol affects the function of a multitude of other ion channels[7–10] and metabotropic receptors (serotonin, cholinergic, and glutamate receptors).[11–13]

Ethanol has also been shown to cause brain and eye defects by interfering with expression of key developmental transcription factor (*Pax6*, *Otx2*, etc.),[19,50,74] retinoic acid signaling,[14–16] and reactive oxygen and nitrogen species signaling.[17–20] Thus, the effect of ethanol is likely to be multipronged, synergistically culminating in fetal alcohol syndrome-associated brain and eye defects. These different mechanisms of ethanol may be triggered during different developmental time points between stages 9–40. In such a case, the maximum additive/synergistic effect of ethanol will be seen only when ethanol exposure happens throughout stages 9–40. Partial exposure may trigger only a small subset of these mechanisms, which may or may not be sufficient to cause mispatterning of the brain and eye.

We have successfully exploited blue light-induced hyperpolarization via ChR2[D156A] to rescue tadpoles from ethanol-induced brain and eye patterning defects (Fig. 2 and 5). Exposure to blue light alone or *β-galactosidase* mRNA injection and blue light exposure failed to rescue embryos from the ethanol effect (Fig. 2E), suggesting that the rescue is due to specific action of ChR2[D156A] activation.

Temporal modulation of membrane voltage showed that hyperpolarization was necessary for the full duration of ethanol exposure (stage 9–40), and shorter durations (stage 9–23 and stage 23–40) were insufficient to rescue the tadpoles from ethanol-induced brain and eye morphology defects (Fig. 3). This suggests that perhaps hyperpolarization is actively countering the effect of ethanol and is therefore required for the same duration as ethanol. This is supported by the observation that one potential target of ethanol is the channel Kir2.1.[5]

Inhibition of the Kir2.1 channel by ethanol would depolarize the cells, but optogenetic hyperpolarization should counter that action of ethanol; however, we provided blue light exposure from stage 9–23 with ethanol exposure from 9 to 40, a regimen that is theoretically equivalent to ethanol exposure from stage 23–40. As seen in Figure 1, a shorter exposure to ethanol should cause much fewer neural defects than we actually observed. Second, we see that optogenetic hyperpolarization of noncell autonomous locations can still rescue brain and eye patterning defects over long range (Fig. 4). These observations suggest that direct antagonism of ethanol action by optogenetic hyperpolarization is not the only possible mechanism, and complex interactions with multiple ethanol targets may be in play.

As mentioned above, ethanol acts via multiple different mechanisms, from effects on retinoic acid signaling, reactive oxygen and nitrogen species, ion channels, metabotropic receptors, and so on.[6,7,12,13,18,20] However, it is interesting to note that a majority of these pathways converge on expression patterns of canonical gene transcription factors such as *Otx2* and *Pax6*, which are critical for proper neural patterning.[19,50,74] Bioelectric signals during embryonic development act upstream of these transcription factors and can be used to even induce these transcription factors

ectopically within the developing embryo.[24,32,34] Moreover, enforcing these bioelectrical signals has been shown to correct misexpression of these transcription factors caused by mutated notch signals or teratogens such as nicotine.[34,42] Hence, it is conceivable that ethanol-induced misexpression (via combination of its various mechanisms) of such crucial transcription factors is overridden by bioelectric regulation of these crucial gene regulatory networks[27] without even interfering with ethanol targets. Further work will be needed to test this hypothesis.

To understand whether optogenetic rescue of ethanol-induced brain and eye phenotypes occurs in a local or non-local mechanism, we introduced the optogenetic channel specifically in dorsal (neural precursors) or ventral (distant) tissues of the embryos, thus restricting our optogenetic hyperpolarization to those respective tissues. Optogenetic hyperpolarization of neural precursors (local effect) was able to rescue ethanol-induced brain and eye morphology defects (Fig. 4), again suggesting a cell autonomous direct antagonism of ethanol. Interestingly, however, noncell autonomous (distant effect) optogenetic hyperpolarization not only rescued ethanol-induced brain and eye defects but did so to a greater degree, resulting in complete rescue (Fig. 4). This observation means that in addition to the possible cell autonomous antagonism of ethanol effect, there is another, perhaps stronger, noncell autonomous mechanism at play.

Noncell autonomous, long-range control of anatomical patterning is seen throughout various aspects of biology. Instructive signals from distant regions have been shown to control macrophage-mediated zebrafish pigment patterning,[75] amphibian trunk and tail development[76] and regeneration,[77] coordinated limb development in mice,[78] deer antler patterning,[79,80] head/tail determination in planarian regeneration,[81] and cancer.[82,83] During embryonic development, it is likely that any individual organ patterning is coordinated with the patterning of other organs and with whole-body morphogenesis and patterning.

For embryonic brain and eye development, membrane voltage patterns of *both* neural (dorsal) and non-neural (ventral) regions are critical regulators of neural patterning.[33,34] Long-range non-neural (ventral) membrane voltage patterns also regulate neural tube cell behaviors (proliferation and apoptosis).[33,34] This long-range effect is partly mediated by signaling through gap-junctions, but other aspects of this signaling remain as yet undiscovered.

The non-neural (ventral) membrane voltage signal could be relayed due to ectodermal cohesion during neurulation.[84,85] Given that the distant (ventral) tissues are intimately involved in neural patterning and morphogenesis, it is possible that the membrane voltage signals from ventral tissues can compensate for or override deficits in neural tissue patterning. This is an area of active investigation.

Conclusion

Endogenous membrane voltage patterns in neurula stage *Xenopus* embryos are critical regulators of brain and eye patterning.[32–35] We know that abnormal signals can be overridden to rescue neural defects using bioelectric signal modulation.[34,42] To determine the spatial and temporal requirements for bioelectric interventions, we tested the ability of optogenetically initiated bioelectric signals to rescue

ethanol-induced teratogenic brain and eye morphology defects. Blue light-mediated activation of ChR2[D156A] channels, to hyperpolarize membrane voltage, rescued ethanol-induced brain and eye morphology defects. This bioelectric intervention was necessary for the full duration of ethanol exposure and works locally and/or at a distance. At present, there are a number of ion channel modulators prescribed to pregnant women for various conditions.[86–88] These same already used ion channel modulators could be studied, investigated, and potentially co-opted for their ability to rescue brain- and eye-related birth defects.

Author Contributions

V.P.P. contributed to the experimental design, performed experiments, and wrote the article. D.S.A. contributed to the experimental design and edited the article.

Author Disclosure Statement

No competing financial interests exist.

References

1. Copp AJ, Greene ND. Genetics and development of neural tube defects. J Pathol 2010;220:217–230.
2. Parrini E, Conti V, Dobyns WB, et al. Genetic basis of brain malformations. Mol Syndromol 2016;7:220–233.
3. May-Simera H, Liu C. Neuronal Polarity and Neurological Disorders. J Neurol Transl Neurosci 2013;2:1026.
4. Muralidharan P, Sarmah S, Zhou FC, et al. Fetal alcohol spectrum disorder (FASD) associated neural defects: Complex mechanisms and potential therapeutic targets. Brain Sci 2013;3:964–991.
5. Bates EA. A potential molecular target for morphological defects of fetal alcohol syndrome: Kir2.1. Curr Opin Genet Dev 2013;23:324–329.
6. Fainsod A, Kot-Leibovich H. Xenopus embryos to study fetal alcohol syndrome, a model for environmental teratogenesis. Biochem Cell Biol 2018;96:77–87.
7. Crews FT, Morrow A.L, Criswell H, et al. Effects of ethanol on ion channels. Int Rev Neurobiol 1996;39:283–367.
8. Bukiya AN, Kuntamallappanavar G, Edwards J, et al An alcohol-sensing site in the calcium- and voltage-gated, large conductance potassium (BK) channel. Proc Natl Acad Sci U S A 2014;111:9313–9318.
9. Oz M, Tchugunova Y, Dinc M. Inhibition of cromakalim-activated K+ current by ethanol in follicle-enclosed Xenopus

oocytes. Naunyn Schmiedebergs Arch Pharmacol 2003;367: 80–85.

10. Clayton R, woodward JJ. Effects of ethanol on three endogenous membrane conductances present in *Xenopus laevis* oocytes. Neurochem Int 1999;36:67–74.

11. Minami K, Gereau RWT, Minami M, et al. Effects of ethanol and anesthetics on type 1 and 5 metabotropic glutamate receptors expressed in *Xenopus laevis* oocytes. Mol Pharmacol 1998;53:148–156.

12. Aoshima H, Hossain SJ, Hamamoto K, et al. Kinetic analyses of alcohol-induced potentiation of the response of GABA(A) receptors composed of alpha(1) and beta(1) subunits. J Biochem 2001;130:703–709.

13. Sanna E, Dildy-Mayfield JE, Harris RA. Ethanol inhibits the function of 5-hydroxytryptamine type 1c and muscarinic M1 G protein-linked receptors in Xenopus oocytes expressing brain mRNA: Role of protein kinase C. Mol Pharmacol 1994;45:1004–1012.

14. Shukrun N, Shabtai Y, Pillemer G, et al. Retinoic acid signaling reduction recapitulates the effects of alcohol on embryo size. Genesis 2019;57:e23284.

15. Shabtai Y, Fainsod A. Competition between ethanol clearance and retinoic acid biosynthesis in the induction of fetal alcohol syndrome. Biochem Cell Biol 2018;96:148–160.

16. Kot-Leibovich H, Fainsod A. Ethanol induces embryonic malformations by competing for retinaldehyde dehydrogenase activity during vertebrate gastrulation. Dis Model Mech 2009;2:295–305.

17. Peng Y, Yang PH, Ng SS, et al. Protection of *Xenopus laevis* embryos against alcohol-induced delayed gut maturation and growth retardation by peroxiredoxin 5 and catalase. J Mol Biol 2004;340:819–827.

18. Peng Y, Yang PH, Guo Y, et al. Catalase and peroxiredoxin 5 protect Xenopus embryos against alcohol-induced ocular anomalies. Invest Ophthalmol Vis Sci 2004;45:23–29.

19. Peng Y, Yang PH, Ng SS, et al. A critical role of Pax6 in alcohol-induced fetal microcephaly. Neurobiol Dis 2004; 16:370–376.

20. Zhang Y, Wang H, Li Y, et al. A review of interventions against fetal alcohol spectrum disorder targeting oxidative stress. Int J Dev Neurosci 2018;71:140–145.

21. Nuccitelli R. Endogenous electric fields in embryos during development, regeneration and wound healing. Radiat Prot Dosimetry 2003;106:375–383.

22. Jaffe LF. Control of development by steady ionic currents. Fed Proc 1981;40:125–127.

23. McCaig CD, Rajnicek AM, Song B, et al. Controlling cell behavior electrically: Current views and future potential. Physiol Rev 2005;85:943–978.

24. Adams DS, Uzel SG, Akagi J, et al. Bioelectric signalling via potassium channels: A mechanism for craniofacial dysmorphogenesis in KCNJ2-associated Andersen-Tawil Syndrome. J Physiol 2016;594:3245–3270.

25. Levin M. Molecular bioelectricity in developmental biology: New tools and recent discoveries: Control of cell behavior and pattern formation by transmembrane potential gradients. Bioessays 2012;34:205–217.

26. Levin M. Reprogramming cells and tissue patterning via bioelectrical pathways: Molecular mechanisms and biomedical opportunities. Wiley Interdiscip Rev Syst Biol Med 2013;5:657–676.

27. Pai VP, Martyniuk CJ, Echeverri K, et al. Genome-wide analysis reveals conserved transcriptional responses down-

stream of resting potential change in Xenopus embryos, axolotl regeneration, and human mesenchymal cell differentiation. Regeneration (Oxf) 2016;3:3–25.

28. Pai VP, Levin M. Chapter 5: Bioelectric control of stem cell function. In: Calegari F, Waskov C, eds. Stem Cells: From Basic Research to Therapy. Vol 1. Chapter 5. Boca Raton, FL: CRC Press, 2014: 106–148.

29. Kim JB. Channelopathies. Korean J Pediatr 2014;57:1–18.

30. Adams DS, Levin M. General principles for measuring resting membrane potential and ion concentration using fluorescent bioelectricity reporters. Cold Spring Harb Protoc 2012;2012:385–397.

31. Vandenberg LN, Morrie RD, Adams DS. V-ATPase-dependent ectodermal voltage and pH regionalization are required for craniofacial morphogenesis. Dev Dyn 2011; 240:1889–1904.

32. Pai VP, Aw S, Shomrat T, et al. Transmembrane voltage potential controls embryonic eye patterning in *Xenopus laevis*. Development 2012;139:313–323.

33. Pai VP, Lemire JM, Chen Y, et al. Local and long-range endogenous resting potential gradients antagonistically regulate apoptosis and proliferation in the embryonic CNS. Int J Dev Biol 2015;59:327–340.

34. Pai VP, Lemire JM, Pare JF, et al. Levin Endogenous gradients of resting potential instructively pattern embryonic neural tissue via Notch signaling and regulation of proliferation. J Neurosci 2015;35:4366–4385.

35. Pai VP, Vandenberg LN, Blackiston D, et al. Neurally derived tissues in *Xenopus laevis* embryos exhibit a consistent bioelectrical left-right asymmetry. Stem Cells Int 2012;2012:353491.

36. Bronner ME. Formation and migration of neural crest cells in the vertebrate embryo. Histochem Cell Biol 2012;138: 179–186.

37. Bronner ME, Simões-Costa M. The neural crest migrating into the twenty-first century. Curr Top Dev Biol 2016;116: 115–134.

38. Stone LS. Experiments on the transplantation of placodes of the cranial ganglia in the amphibian embryo I. Heterotopic transplantations of the ophthalmic placode upon the head of Amblystoma punctatum. J Comp Neurol 1924;38: 73–105.

39. Adameyko I, Fried K. The nervous system orchestrates and integrates craniofacial development: A review. Front Physiol 2016;7:49.

40. Moody SA, Peterson MC, Xu JN, et al. The molecular regulation of cranial placode specification. FASEB J 2011; 25:184.1.

41. Schlosser G, Awtry T, Brugmann SA, et al. Eya1 and Six1 promote neurogenesis in the cranial placodes in a SoxB1-dependent fashion. Dev Biol 2008;320:199–214.

42. Pai VP, Pietak A, Willocq V, et al. HCN2 Rescues brain defects by enforcing endogenous voltage pre-patterns. Nat Commun 2018;9:998.

43. Herrera-Rincon C, Pai VP, Moran KM, et al. The brain is required for normal muscle and nerve patterning during early Xenopus development. Nat Commun 2017;8:587.

44. Fenno L, Yizhar O, Deisseroth K. The development and application of optogenetics. Annu Rev Neurosci 2011;34: 389–412.

45. Knopfel T, Lin MZ, Levskaya A, et al. Toward the second generation of optogenetic tools. J Neurosci 2010;30:14998–15004.

46. Liu X, Tonegawa S. Optogenetics 3.0. Cell 2010;141:22–24.

47. Adams DS, Tseng AS, Levin M. Light-activation of the Archaerhodopsin H(+)-pump reverses age-dependent loss of vertebrate regeneration: Sparking system-level controls in vivo. Biol Open 2013;2:306–313.

48. Chernet BT, Adams DS, Lobikin M, et al. Use of genetically encoded, light-gated ion translocators to control tumorigenesis. Oncotarget 2016;7:19575–19588.

49. Nakatsuji N. Craniofacial malformation in *Xenopus laevis* tadpoles caused by the exposure of early embryos to ethanol. Teratology 1983;28:299–305.

50. Yelin R, Kot H, Yelin D, et al. Early molecular effects of ethanol during vertebrate embryogenesis. Differentiation 2007;75:393–403.

51. Sive H, Grainger RM, Harland R. Early Development of *Xenopus laevis*. Cold Spring Harbor, New York: Cold Spring Harbor Laboratory Press, 2000: 338.

52. Nieuwkoop PD, Faber J. Normal Table of *Xenopus laevis* (Daudin): A Systematical and Chronological Survey of the Development from the Fertilized Egg Till the end of Metamorphosis. New York: Garland Pub, 1994: 252.

53. Zahn N, Levin M, Adams DS. The Zahn drawings: New illustrations of Xenopus embryo and tadpole stages for studies of craniofacial development. Development 2017; 144:2708–2713.

54. Pratt KG, Khakhalin AS. Modeling human neurodevelopmental disorders in the Xenopus tadpole: From mechanisms to therapeutic targets. Dis Model Mech 2013;6: 1057–1065.

55. Bamann C, Gueta R, Kleinlogel S, et al. Structural guidance of the photocycle of channelrhodopsin-2 by an interhelical hydrogen bond. Biochemistry 2010;49:267–278.

56. Lorenz-Fonfria VA, Heberle J. Channelrhodopsin unchained: Structure and mechanism of a light-gated cation channel. Biochim Biophys Acta 2014;1837:626–642.

57. Adams DS, Lemire JM, Kramer RH, et al. Optogenetics in developmental biology: Using light to control ion flux-dependent signals in Xenopus embryos. Int J Dev Biol 2014;58:851–861.

58. Lin JY, Lin MZ, Steinbach P, et al. Characterization of engineered channelrhodopsin variants with improved properties and kinetics. Biophys J 2009;96:1803–1814.

59. Moody SA. Fates of the blastomeres of the 32-cell-stage Xenopus embryo. Dev Biol 1987;122:300–319.

60. Adams DS, Robinson KR, Fukumoto T, et al. Early, H$^+$-V-ATPase-dependent proton flux is necessary for consistent left-right patterning of non-mammalian vertebrates. Development 2006;133:1657–1671.

61. Aw S, Adams DS, Qiu D, et al. H,K-ATPase protein localization and Kir4.1 function reveal concordance of three axes during early determination of left-right asymmetry. Mech Dev 2008;125:353–372.

62. Adams DS, Levin M. Endogenous voltage gradients as mediators of cell-cell communication: Strategies for investigating bioelectrical signals during pattern formation. Cell Tissue Res 2013;352:95–122.

63. Levin M. Endogenous bioelectrical networks store non-genetic patterning information during development and regeneration. J Physiol 2014;592(Pt 11):2295–2305.

64. Tseng A, Levin M. Cracking the bioelectric code: Probing endogenous ionic controls of pattern formation. Commun Integr Biol 2013;6:e22595.

65. Mathews J, Levin M. The body electric 2.0: Recent advances in developmental bioelectricity for regenerative and synthetic bioengineering. Curr Opin Biotechnol 2018;52: 134–144.

66. Kozorovitskiy Y, Saunders A, Johnson CA, et al. Recurrent network activity drives striatal synaptogenesis. Nature 2012;485:646–650.

67. Penn AA, Shatz CJ. Brain waves and brain wiring: The role of endogenous and sensory-driven neural activity in development. Pediatr Res 1999;45(4 Pt 1):447–458.

68. Beane WS, Morokuma J, Lemire JM, et al. Bioelectric signaling regulates head and organ size during planarian regeneration. Development 2013;140:313–322.

69. Hempel A, Kuhl M. A matter of the heart: The African clawed frog xenopus as a model for studying vertebrate cardiogenesis and congenital heart defects. J Cardiovasc Dev Dis 2016;3.

70. Popov S, Venetsanou K, Chedrese PJ, et al. Bertorello Increases in intracellular sodium activate transcription and gene expression via the salt-inducible kinase 1 network in an atrial myocyte cell line. Am J Physiol Heart Circ Physiol 2012;303:H57–H65.

71. Huang BS, White RA, Leenen FH. Possible role of brain salt-inducible kinase 1 in responses to central sodium in Dahl rats. Am J Physiol Regul Integr Comp Physiol 2012; 303:R236–R245.

72. Allahverdi A, Chen Q, Korolev N, et al. Chromatin compaction under mixed salt conditions: Opposite effects of sodium and potassium ions on nucleosome array folding. Sci Rep 2015;5:8512.

73. Lin JY, Lin MZ, Steinbach P, et al. Characterization of engineered channelrhodopsin variants with improved properties and kinetics. Biophys J 2009;96:1803–1814.

74. Yelin R, Schyr RB, Kot H, et al. Ethanol exposure affects gene expression in the embryonic organizer and reduces retinoic acid levels. Dev Biol 2005;279:193–204.

75. Eom DS, Parichy DM. A macrophage relay for long-distance signaling during postembryonic tissue remodeling. Science 2017;355:1317–1320.

76. Mondia JP, Levin M, Omenetto FG, et al. Long-distance signals are required for morphogenesis of the regenerating Xenopus tadpole tail, as shown by femtosecond-laser ablation. PLoS One 2011;6:e24953.

77. Kumar A, Brockes JP. Nerve dependence in tissue, organ, and appendage regeneration. Trends Neurosci 2012;35: 691–699.

78. Rosello-Diez A, Madisen L, Bastide S, et al. Cell-nonautonomous local and systemic responses to cell arrest enable long-bone catch-up growth in developing mice. PLoS Biol 2018;16:e2005086.

79. Marburger RG, Robinson RM, Thomas JW, et al. Antler malformation produced by leg injury in white-tailed deer. J Wildl Dis 1972;8:311–314.

80. Acharjyo LN, Misra R. Effects of amputation of a hind limb on the growth of antlers of deer in captivity. Indian Forester 1972;98:507–508.

81. Oviedo NJ, Morokuma J, Walentek P, et al. Long-range neural and gap junction protein-mediated cues control polarity during planarian regeneration. Dev Biol 2010;339: 188–199.

82. Chernet BT, Fields C, Levin M. Long-range gap junctional signaling controls oncogene-mediated tumorigenesis in *Xenopus laevis* embryos. Front Physiol 2014;5:519.

83. Lobikin M, Chernet B, Lobo D, et al. Resting potential, oncogene-induced tumorigenesis, and metastasis: The bioelectric basis of cancer in vivo. Phys Biol 2012;9:065002.

84. Levine E, Lee CH, Kintner C, et al. Selective disruption of E-cadherin function in early Xenopus embryos by a dominant negative mutant. Development 1994;120:901–909.

85. Nandadasa S, Tao Q, Menon NR, et al. N- and E-cadherins in Xenopus are specifically required in the neural and non-neural ectoderm, respectively, for F-actin assembly and morphogenetic movements. Development 2009;136:1327–1338.

86. Goldsmith DR, Wagstaff AJ, Ibbotson T, et al. Lamotrigine: A review of its use in bipolar disorder. Drugs 2003;63:2029–2050.

87. Dolk H, Wang H, Loane M, et al. Lamotrigine use in pregnancy and risk of orofacial cleft and other congenital anomalies. Neurology 2016;86:1716–1725.

88. Wiffen PJ, Derry S, Bell RF, et al. Gabapentin for chronic neuropathic pain in adults. Cochrane Database Syst Rev 2017;6:CD007938.

Address correspondence to:
Dany Spencer Adams, PhD
Ion Diagnostics LLC
200 Dexter Avenue, ste 260
Watertown, MA 02472

Email: adams@ion-diagnostics.com